

## Experimental Physiology

# Double-sigmoid model for fitting fatigue profiles in mouse fast- and slow-twitch muscle

S. P. Cairns<sup>1</sup>, D. M. Robinson<sup>2,3</sup> and D. S. Loiselle<sup>2,4</sup>

<sup>1</sup>Institute of Sport and Recreation Research New Zealand, Faculty of Health and Environmental Science, AUT University, Auckland 1020, New Zealand

<sup>2</sup>Department of Physiology, School of Medicine and <sup>4</sup>Bioengineering Institute, University of Auckland, Auckland 92019, New Zealand

<sup>3</sup>Wolters Kluwer Health Adis, North Shore 0754, Auckland, New Zealand

We present a curve-fitting approach that permits quantitative comparisons of fatigue profiles obtained with different stimulation protocols in isolated slow-twitch soleus and fast-twitch extensor digitorum longus (EDL) muscles of mice. Profiles from our usual stimulation protocol (125 Hz for 500 ms, evoked once every second for 100–300 s) could be fitted by single-term functions (sigmoids or exponentials) but not by a double exponential. A clearly superior fit, as confirmed by the Akaike Information Criterion, was achieved using a double-sigmoid function. Fitting accuracy was exceptional; mean square errors were typically  $<1\%$  and  $r^2 > 0.9995$ . The first sigmoid (early fatigue) involved  $\sim 10\%$  decline of isometric force to an intermediate plateau in both muscle types; the second sigmoid (late fatigue) involved a reduction of force to a final plateau, the decline being 83% of initial force in EDL and 63% of initial force in soleus. The maximal slope of each sigmoid was seven- to eightfold greater in EDL than in soleus. The general applicability of the model was tested by fitting profiles with a severe force loss arising from repeated tetanic stimulation evoked at different frequencies or rest periods, or with excitation via nerve terminals in soleus. Late fatigue, which was absent at 30 Hz, occurred earlier and to a greater extent at 125 than 50 Hz. The model captured small changes in rate of late fatigue for nerve terminal *versus* sarcolemmal stimulation. We conclude that a double-sigmoid expression is a useful and accurate model to characterize fatigue in isolated muscle preparations.

(Received 5 November 2007; accepted after revision 10 March 2008; first published online 14 March 2008)

**Corresponding author** S. P. Cairns: School of Sport and Recreation, AUT University, Private Bag 92006, Auckland 1020, New Zealand. Email: simeon.cairns@aut.ac.nz

Lännergren & Westerblad (1991) were the first to describe carefully the fatigue profile obtained with repeated tetani in isolated single fast-twitch muscle fibres from mice. They identified three phases of fatigue: a moderate initial decline of peak force (phase I), followed by a period of relatively steady force (phase II), leading to a late decline of force (phase III). However, the appearance of these phases is not universal and may depend on the fatigue model employed (Cairns *et al.* 2005). The phases may be influenced by the stimulation regime, being less obvious with short rest periods between tetani (Chin & Allen, 1998; Ward *et al.* 1998) or with high stimulation frequencies (Bevan *et al.* 1992; Cairns *et al.* 2004), and many studies have not used extended stimulation periods (Lindinger & Heigenhauser, 1988; Lännergren & Westerblad, 1991; Clausen *et al.* 2004) so that late changes may have been missed. The phases

may also depend on the site of excitation, for example via nerve terminals *versus* the sarcolemma of muscle fibres (Cairns *et al.* 2007). Importantly, the profile may vary with the muscle fibre-type composition of the motor unit or muscle studied, since the original description was only for fast-twitch fibres (Lännergren & Westerblad, 1991). Indeed, the classical work of Burke *et al.* (1973) shows that these phases exist with repeated tetanic stimulation of fast fatigue-resistant (FR) motor units, but not with fast fatiguable (FF) or slow (S) motor units.

Many studies have quantified fatigue using a fatigue index represented by the peak force at a defined stimulation time (or tetanus number) relative to that of the first contraction (Burke *et al.* 1973; Juel, 1986; Mizrahi *et al.* 1997; Chen *et al.* 2001). This approach reveals the extent of fatigue but information about the time course of fatigue

is necessarily lost. For example, fatigue induced with repeated tetani has an earlier onset, but the final extent is the same, at low extracellular chloride (Cairns *et al.* 2004) or with various sarcolemmal ion channel blockers (Gong *et al.* 2003; Kristensen *et al.* 2006). Also, in the study of Burke *et al.* (1973) the fatigue index at 2 min of stimulation showed that the force decline was greater in FF than FR motor units, yet the FF motor units were resistant to the early fatigue (see their Fig. 1F) seen in FR motor units (see their Fig. 2F).

In order to extract information about the rate(s) and extent(s) of fatigue there have been several attempts to curve-fit the entire fatigue profile from isolated animal muscles or human muscle *in vivo*. Such studies have involved straight-line regression (Merletti *et al.* 1991; Clausen *et al.* 2004), single-exponential models (Merletti *et al.* 1991; Rabischong & Chavet, 1997; Nagaraj *et al.* 2000) or the equivalent logarithmic transformations (Williams & Ward, 1991), single-sigmoid models with a four-parameter Hill equation (Russ *et al.* 2002), two exponential functions with ascending followed by descending exponential curves (Boom *et al.* 1993; Mizrahi *et al.* 1997) and a fourth-order polynomial (Merletti *et al.* 1991). These models have shown variable ability to fit the entire fatigue profile, and most models are inadequate when multiple phases are present. Moreover, the use of curve-fitting to provide quantitative information on the time course or rate(s) of fatigue in fast-twitch *versus* slow-twitch muscles is surprisingly limited (Clausen *et al.* 2004).

There is a need to quantify carefully the rate and extent of each phase of fatigue to assist investigation of mechanisms, since early fatigue is postulated to be due to impaired maximal cross-bridge function and late fatigue to reduced  $\text{Ca}^{2+}$  release from the sarcoplasmic reticulum (SR; Lännergren & Westerblad, 1991; Chin & Allen, 1998; Dahlstedt *et al.* 2000). Moreover, mouse muscles are particularly relevant, since the mouse is the animal of choice for molecular biology interventions (Dahlstedt *et al.* 2000; Nagaraj *et al.* 2000; Chen *et al.* 2001; Chin *et al.* 2003; Gong *et al.* 2003). Therefore, the main aims of the present study were to establish the best curve-fitting approach to obtain detailed quantitative descriptions of profiles of severe fatigue induced with repeated brief tetani in isolated skeletal muscle of mice, and to apply this methodology to quantify differences in fatigue profiles of fast-twitch and slow-twitch muscles.

## Methods

### Muscle preparations and solutions

Female Swiss CD-1 mice, 4–12 weeks of age and weighing 20–35 g, were killed by cervical dislocation and their hindlimbs removed. Intact soleus or EDL muscles were then dissected in Krebs solution (composition,

mm: 122.2 NaCl, 2.8 KCl, 1.2  $\text{KH}_2\text{PO}_4$ , 25.1  $\text{NaHCO}_3$ , 1.2  $\text{MgSO}_4$ , 1.3  $\text{CaCl}_2$  and 5 D-glucose) which was bubbled with 95%  $\text{O}_2$ –5%  $\text{CO}_2$  at room temperature (21–23°C). All studies were approved by the Animal Ethics Committee of the University of Auckland.

### Stimulation and isometric force recording

The experimental set-up has been described in considerable detail elsewhere (Cairns *et al.* 2007). In brief, muscles were mounted vertically by their tendons in a chamber containing ~100 ml of Krebs solution (bubbled with 95%  $\text{O}_2$ –5%  $\text{CO}_2$ ) and immersed in a temperature-controlled bath at 25°C. Isometric force was measured using a semiconductor strain gauge (KSP-2-E3, Kyowa, Japan). Contractions were evoked by electric field stimulation, delivered via two parallel plate platinum electrodes which flanked the muscle. The standard bipolar rectangular pulses (20 V, 0.1 ms) were supramaximal for the twitch. Twitches and tetani were initiated from an Apple Macintosh PowerPC 7100/80 using custom-written Labview software. Contractions were recorded continuously on a chart recorder (Gould model 244) with selected contractions saved in digital form. The force data obtained during fatiguing stimulation were measured from chart recordings.

The preliminary protocol involved adjusting muscle length until maximal tetanic force was achieved, followed by 30–60 min equilibration during which tetani were evoked every 5 min. In order to generate maximal force, the muscles were stimulated at 125 Hz for 2 s in soleus and at 200 Hz for 0.5 s in EDL. In the present study, fatigue is defined as any reversible decline of peak tetanic force evoked by repeated electrical stimulation of muscle. The fatiguing stimulation regime we most commonly used involved brief tetani (125 Hz for 500 ms), with one contraction repeated each second for 100 s; this stimulation regime was used to compare fatigue profiles between muscle types. These tetani evoked  $93.8 \pm 0.5$  ( $n = 32$ ) or  $91.3 \pm 0.5\%$  ( $n = 13$ ) of maximal force in soleus and EDL, respectively. Other stimulation regimes involved changing the stimulus frequency, rest period duration, number of contractions or the pulse parameters, but in each case there was a constant inter-train interval. After each fatigue run (i.e. a single stimulation episode consisting of 20–300 tetani), the peak force was monitored until maximal recovery occurred to ensure that the prior diminution of force had not been due to irreversible deterioration of the muscle. Two criteria were used to ensure that a muscle was healthy prior to the start of the first fatigue run. Those muscles whose peak tetanic force: (1) diminished at a rate greater than  $2\% \text{ min}^{-1}$ ; or (2) evoked with 1.0 ms pulses was 20% greater than that evoked with 0.1 ms pulses, were rejected on the basis of submaximal excitation.

## Analysis of force records

The contractile parameters measured were peak twitch and tetanic force, and fade. Fade was calculated as the ratio of the force at the end of a 500 ms tetanus relative to the peak force achieved during that tetanus. Post-tetanic potentiation or inhibition of twitches was assessed as the average peak force of two consecutive twitches recorded 10–15 s after a tetanus expressed relative to that for twitches recorded prior to the tetanus (3–4 min after the previous tetanus).

**Fatigue parameters.** The peak force of a tetanus during a fatigue run was normalized to the maximal force generated during a non-fatigued 500 ms tetanus at the start of the fatigue run (i.e. to the first or second tetanus). Relative force was calculated for each of the first 10 tetani, then every fifth tetanus to 100 tetani, followed by every twentieth tetanus to 300 tetani, and included both the evoked force and the resting force. The fatigue profile is depicted as the peak tetanic force (%) expressed as a function of stimulation time. We define a fatigue index (FI) as the relative force at a given time (or, equivalently, tetanus number). For example,  $FI_{100}$  is the fatigue index for the hundredth tetanus. Any change of resting force during a fatigue run was expressed as a percentage of the peak force in the first tetanus.

**Recovery parameters.** Tetani were evoked every 5 min after the cessation of a fatigue run. The peak force for a maximal tetanus was normalized to that of a similar contraction obtained 5 min prior to the start of the fatigue run in non-fatigued muscle. The recovery profile is depicted as the relative force (%) as a function of recovery time.

## Curve-fitting procedures

The relationship between the relative peak tetanic force (%) and time,  $F(t)$ , was fitted using the least-squares, multivariate secant method of non-linear parameter estimation (NLIN) available in the SAS statistical software package. The quantitative basis for choosing the ‘best’ model was examined using the Akaike Information Criterion (AIC), as developed by Burnham & Anderson (1998). This procedure is based on the concept of maximum likelihood and is ideal for ranking a set of non-hierarchical models having variable numbers of fitting parameters. The logic of the AIC procedure was applied as follows. Each of five distinct models was fitted to averaged data sets obtained with various fatigue protocols. Such fitting was first undertaken using a data set, comprising  $N = 190 F(t)$  points arising from five soleus muscles stimulated at 50 Hz intermittently for 300 s, since with this stimulation regime multiple phases are apparent

(see Fig. 1). Fitting using the NLIN procedure of SAS yielded both the parameter estimates and the Mean Square Error ( $MS_\epsilon$ ), calculated according to the usual criterion of minimizing the sum of squared deviations between measured and predicted values of  $F(t)$ . The  $MS_\epsilon$  was then converted to the maximum likelihood estimate of the variance ( $ML_\epsilon$ ) as follows:

$$ML_\epsilon = \frac{(N - K + 1)}{N} MS_\epsilon \quad (1)$$

where  $K = (p + 1)$ ,  $p$  being the number of fitting parameters and ‘+1’ accounting for the additional loss of a degree of freedom due to the need to estimate the variance but not the intercept, which was given by  $F(0) = 100$  in every case. The AIC was then calculated as:

$$AIC = N \ln(ML_\epsilon) + 2K \quad (2)$$

This criterion was then used to rank the five models that we examined. Note that the smaller the value of AIC in eqn (2), the better the fit of the model to the data.

The five models were defined as follows (eqns (3)–(7)) for  $t \geq 0$ . Note that the symbol  $\tau$  is adopted for the three sigmoidal expressions as well as for the two exponential expressions. In the latter case, the symbol denotes the usual time constant (i.e. the time required for  $F(t)$  to fall to  $e^{-1}$  of its initial value). For the three sigmoidal expressions, it denotes the half-time (i.e. the time required for  $F(t)$  to fall to one-half of its initial value).

Six-parameter double sigmoid:

$$F(t) = F_{\min} + (100 - F_o) \left/ \left[ 1 + \left( \frac{t}{\tau_1} \right)^{n_1} \right] \right. + (F_o - F_{\min}) \left/ \left[ 1 + \left( \frac{t}{\tau_2} \right)^{n_2} \right] \right. \quad (3)$$

Five-parameter double sigmoid ( $F_o = 88.9$ : for justification see Results,  $F_o$  is described in Fig. 2):

$$F(t) = F_{\min} + (100 - 88.9) \left/ \left[ 1 + \left( \frac{t}{\tau_1} \right)^{n_1} \right] \right. + (88.9 - F_{\min}) \left/ \left[ 1 + \left( \frac{t}{\tau_2} \right)^{n_2} \right] \right. \quad (4)$$

Three-parameter single sigmoid:

$$F(t) = F_{\min} + (100 - F_{\min}) \left/ \left[ 1 + \left( \frac{t}{\tau} \right)^n \right] \right. \quad (5)$$

Four-parameter double exponential:

$$F(t) = F_{\min} + (100 - F_o)e^{-t/\tau_1} + (F_o - F_{\min})e^{-t/\tau_2} \quad (6)$$

Two-parameter single exponential:

$$F(t) = F_{\min} + (100 - F_{\min})e^{-t/\tau} \quad (7)$$

When fitting each model, the relative force was constrained to be 100% at  $t = 0$ . As shown in the Results (Fig. 1

and Table 1), the best fit of  $F(t)$  was achieved using a double-sigmoid expression, i.e. eqn (3). The slope ( $S$ ) of this expression at any time reflects the rate of fatigue, i.e. the rate of decline of force, at that point. It is found by differentiating eqn (3) with respect to time. We report the values of  $S_1$  and  $S_2$ , the slopes at the half-times of each sigmoid, i.e.  $\tau_1$  and  $\tau_2$ , respectively (see Fig. 2). Equation (8) gives  $S_1$ , the slope at  $\tau_1$ ; an equivalent expression gives the slope at  $\tau_2$ . Note that the fitting parameters  $n_1$  and  $n_2$  determine the maximal slopes of the two sigmoidal components (which occur at  $\tau_1$  and  $\tau_2$ , respectively) although the slope at any time point depends on the value of all the other curve-fitting parameters.

$$S_1 \equiv \frac{\partial F(\tau_1)}{\partial t} = -(100 - F_o) \frac{n_1}{4\tau_1} - (F_o - F_{\min}) \times \frac{n_2}{\tau_2} \frac{\left(\frac{\tau_1}{\tau_2}\right)^{n_2-1}}{\left[1 + \left(\frac{\tau_1}{\tau_2}\right)^{n_2}\right]^2} \quad (8)$$

The standard error (s.e.m.) of  $S_1$  was calculated (as for any derived quantity) as follows:

$$\text{s.e.m.}_{S_1} = \sqrt{\sum_{i=1}^p \sigma_{p_i}^2 \cdot \left(\frac{\partial S_1}{\partial p_i}\right)^2} \quad (9)$$

where  $p_i$  is the  $i^{\text{th}}$  fitting parameter. For the double sigmoid (eqn (3)), in which  $p=6$ , the summation in eqn (9) produces 13 separate terms, each of which is by itself lengthy, so is not presented here, but is available upon request. A similar expression provides the s.e.m. for  $S_2$ .

It is frequently instructive to determine the time at which one of the sigmoids in eqn (3) has declined to some given proportion of its initial value. If this proportion is denoted by  $x$  (where  $0 < x < 1$ ), then the time required to reach  $x$  for a specified sigmoid is given by:

$$t_x = \tau (x^{-1} - 1)^{1/n} \quad (10)$$

Once the best model was established, the fitting procedure was applied to data points from single fatigue runs in individual muscles or to the averaged data from  $n$  muscles in order to estimate fitting parameters. In each case, the goodness-of-fit was described statistically using both the squared correlation coefficient ( $r^2$ ) and the  $MS_e$ , which is the average variance of the measured data around the line of best fit.

## Muscle fibre-type assays

**Histochemistry.** It was desirable to establish the fibre-type composition of the soleus and EDL muscles used in the present study, which can vary with strain, sex, age or colony of the animals, in order to relate the composition to the fatigue profiles. Sections were cut

from the central region of muscles, frozen in liquid propane at approximately resting length, and the fibre-type composition confirmed by assays of myosin ATPase activity. For details see Robinson & Loiselle (2002). The slow-twitch type I fibres were acid-stable/alkaline-labile, whereas fast-twitch type II fibres were alkaline-stable/acid-labile, and could be further classified into subtypes based on their relative acid stability at pH 4.5 using histochemical nomenclature (Crow & Kushmerick, 1982; Robinson & Loiselle, 2002; Chin *et al.* 2003). Fibre-type composition was expressed as relative fibre area in the whole muscle cross-section rather than as relative fibre number, to represent better the contribution to mechanical function (Robinson & Loiselle, 2002).

**Morphology.** Muscle sections were digitally captured (Kodak Professional DCS200, Eastman Kodak, Rochester, NY, USA) using Photoshop 2.5 (Adobe Systems, San Jose, CA, USA). A software package, National Institutes of Health Image version 1.57 (NIH, Bethesda, MD, USA) was used to quantify the number of pixels within a narrow range of stain densities that represented a single fibre-type. The number of each type of fibre per muscle was counted manually. The relative fibre area (%) was calculated as the number of pixels identified as a given fibre-type, expressed as a percentage of the total number of pixels in the muscle section. The total fibre area, which reflects muscle cross-sectional area, was calculated as the summed area of all fibres in each muscle section (knowing the area per pixel) averaged over all muscles.

## Statistical analyses

Data in the text are given as the mean values  $\pm$  s.e.m. for the number ( $n$ ) of muscles tested, unless stated otherwise. Statistical analyses involved one-way repeated-measures analyses of variance (ANOVA) performed using SAS software (Sas Institute Inc., Cary, NC, USA). Differences among means were subsequently examined using orthogonal sets of contrast coefficients, thereby ensuring constancy of type I error rate. Differences between fitting parameters, or quantities derived from them, were tested using Student's unpaired  $t$  tests. Statistical significance was taken as  $P < 0.05$ , unless stated otherwise.

## Results

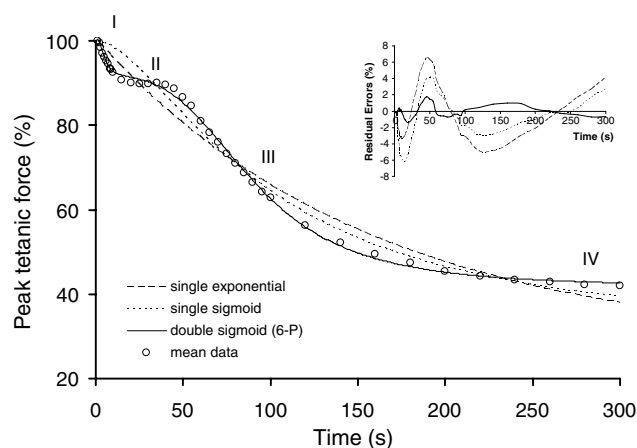
### Curve-fitting to the fatigue profile

Figure 1 shows that the data describing the decline of peak tetanic force in soleus muscles stimulated at 50 Hz for 500 ms once per second for 300 s, were well fitted by a six-parameter double-sigmoid model (i.e. eqn (3)). Numerical details arising from application of the AIC to determine the model of best-fit are summarized in

Table 1, where the superiority of the double-sigmoid models (whether 5- or 6-parameter) is indicated by their lowest values of AIC. Note that it was not possible to achieve convergence using a four-parameter double exponential (eqn (6)). Thus, we conclude that the best analytical model with which to fit these severe fatigue data is one of double-sigmoid form. This conclusion is bolstered by the data shown in the inset of Fig. 1, where it can be seen that the largest residual error associated with the double sigmoid (in absolute value, less than 2%) is less than one-half that arising from a single-sigmoid fit and one-third that from a single-exponential fit.

A schematic representation of such a relationship (eqn (3)), depicting its fitting and derived parameters, is shown in Fig. 2. Parameter  $F_0$  represents the intermediate asymptote jointly shared by the two sigmoidal terms, and  $F_{\min}$  is the minimum asymptote of the function achieved as  $t \rightarrow \infty$ . Each half-time ( $\tau_1$  or  $\tau_2$ ), denotes the time at which the corresponding sigmoid has declined by 50% of its extent. Early fatigue is described by the first sigmoid. Its time course is indexed by  $\tau_1$ , as well as by  $S_1$  – the maximum slope (or rate of decline of force) which occurs at  $\tau_1$ . Its extent is indexed by  $(100 - F_0)$ . Late fatigue, represented by the second sigmoid, has its time course and rate described by  $\tau_2$  and  $S_2$ , respectively, and its extent by  $(F_0 - F_{\min})$ .

We deemed it important to scrutinize further the accuracy of fitting parameter  $F_0$ , since it is responsible for determining the amplitudes of the two sigmoidal components (Fig. 2). We did this in two independent ways.



**Figure 1. Three different models fitted to the relative peak tetanic force as a function of time**

The averaged data (○) arose by subjecting soleus muscles to 50 Hz stimulation for 500 ms, once every second for 300 s ( $n = 5$ ). Supramaximal pulses (20 V, 0.1 ms) and plate electrodes were used. Fitting of single-exponential (dashed line), single-sigmoid (dotted line) or double-sigmoid six-parameter models (continuous line) are shown as smooth curves. The inset shows residual errors arising from curve-fitting; residual errors are consistently smaller for the double-sigmoid fit. The legend applies to both fatigue data and residual errors.

**Table 1. Calculation of the Akaike Information Criterion (AIC) for the models listed as eqns (3)–(7)**

Model	$K$	$MS_e$	$ML_e$	AIC
<b>Soleus, 50 Hz fatigue protocol</b>				
Six-parameter double sigmoid	7	19.33	18.72	570.6
Five-parameter double sigmoid	6	19.49	18.98	571.2
Three-parameter single sigmoid	4	27.85	27.41	637.1
Two-parameter single exponential	3	28.73	28.43	642.0
<b>Soleus, 125 Hz fatigue protocol</b>				
Five-parameter double sigmoid	6	42.64	42.01	1290.4
Three-parameter single sigmoid	4	43.94	43.56	1298.7
Two-parameter single exponential	3	43.42	43.16	1293.6
<b>EDL, 125 Hz fatigue protocol</b>				
Six-parameter double sigmoid	7	12.65	12.39	766.7
Five-parameter double sigmoid	6	12.61	12.40	764.7
Three-parameter single sigmoid	4	18.35	18.17	875.0
Two-parameter single exponential	3	35.20	34.96	1068.7

The models are described by eqns (3)–(7) (see Methods).  $K = p + 1$ , where  $p$  is the number of parameters in the model.  $MS_e$  is the (least squares) variance estimate arising from the SAS non-linear curve-fitting routine; and  $ML_e$  is the maximum likelihood estimate of the variance (eqn (1)). The smaller the AIC (eqn (2)), the greater the likelihood that that model is the best one with which to describe the data set (Burnham & Anderson, 1998). Muscles were stimulated with tetani for 500 ms once every second for 300 s in soleus and 100 s in EDL.

First, we fitted a single sigmoid to the first 45 tetani for the data of soleus at 50 Hz, where a definitive plateau exists (Fig. 1); the relative force was sustained within 2% of the value at 20 s for a further  $28 \pm 2$  s ( $n = 14$ ). This yielded  $F_0 = 88.9 \pm 0.4\%$  and  $\tau = 5.9 \pm 0.2$  s. These

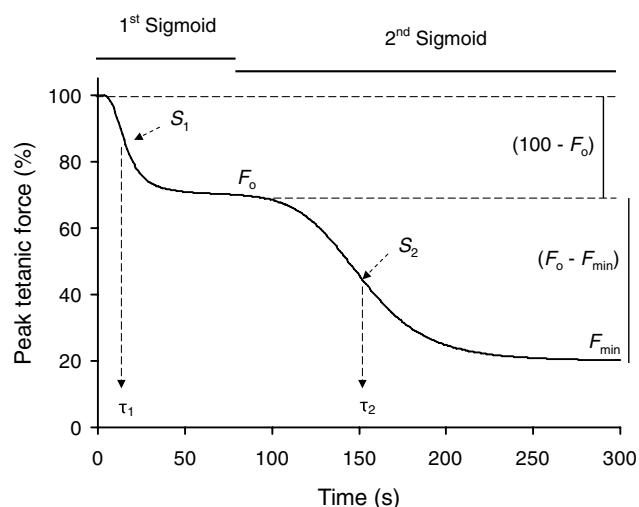


**Figure 2. Schematic presentation of the double-sigmoid model of a fatigue profile, as described by eqn (3)**

Four of the fitting parameters ( $\tau_1$ ,  $F_0$ ,  $\tau_2$  and  $F_{\min}$ ) and four derived parameters ( $S_1$ ,  $S_2$ ,  $(100 - F_0)$  and  $(F_0 - F_{\min})$ ) are shown.  $F_{\min}$  is the minimum asymptote of the function, achieved as  $t \rightarrow \infty$ . The maximal slope of each sigmoid ( $S_1$  and  $S_2$ ), which occurs at  $\tau_1$  and  $\tau_2$ , respectively, is calculated according to eqn (8). Other time course measures (not shown) can be calculated according to eqn (10).

values do not differ significantly from those which arose from fitting the full six-parameter double sigmoid over the full 300 tetani (Table 2). Second, we exploited the observation that a reduction of stimulation frequency from 50 to 30 Hz eliminates the second sigmoidal component that characterizes ‘severe fatigue’ (Fig. 3). Once again, similar parameter values were obtained when a single sigmoid was fitted to the first 45 tetani evoked at 30 Hz;  $F_o = 85.5 \pm 1.0\%$  and  $\tau = 5.6 \pm 0.8$  s. Thus, we subsequently set the value of  $F_o$  at 88.9% whenever it was required to use the five-parameter double-sigmoid model (eqn (4)). Note that use of this value renders the five-parameter model only marginally less efficacious than the six-parameter model (Table 1).

As is evident in Fig. 3, the extent of fatigue increased progressively as the frequency of stimulation was increased from 30 to 50 to 125 Hz. For example, the values of  $FI_{100}$  were  $85 \pm 3\%$  ( $n = 4$ ) at 30 Hz,  $64 \pm 3\%$  ( $n = 14$ ) at 50 Hz and  $36 \pm 3\%$  ( $n = 18$ ) at 125 Hz when tested in the same soleus muscles. With stimulation at 125 Hz for 300 s ( $n = 9$ ), the data were well fitted by a six-parameter double-sigmoid expression ( $r^2 = 0.99998$ ,  $MS_e = 0.07\%$ ). However, the resulting fitting parameters for the first sigmoid ( $F_o = 67.7 \pm 11.0\%$ ,  $\tau_1 = 20.7 \pm 8.5$  s) differed from the earlier estimates and had much greater standard errors. We hypothesized that this lower  $F_o$  arose because the temporal processes underlying the two sigmoids overlapped at 125 Hz. We tested this hypothesis (using eqn (10)) by determining the time difference

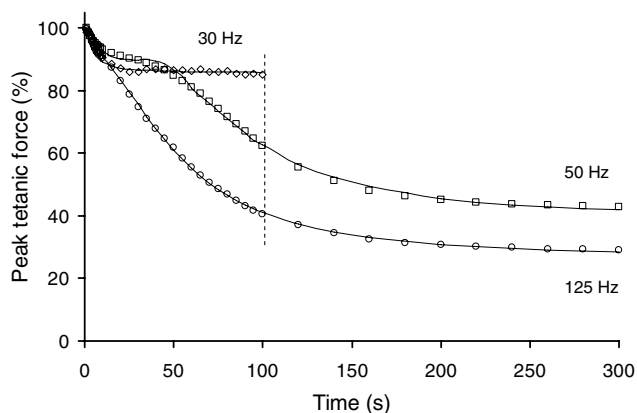


**Figure 3.** Curves fitted to peak tetanic force (%) as a function of time when evoked at different stimulation frequencies in soleus muscle

Stimulation protocol was 30, 50 or 125 Hz for 500 ms, once every second for 100 or 300 s, using supramaximal pulses (20 V, 0.1 ms) and plate electrodes. A single-sigmoid (3-parameter) model was fitted to the mean 30 Hz data over 100 s ( $\diamond$ ,  $n = 4$ ,  $r^2 = 0.99996$ ,  $MS_e = 0.33\%$ ). Double-sigmoid models were fitted to the mean 50 Hz data ( $\square$ ,  $n = 5$ , 6-parameter) and mean 125 Hz data ( $\circ$ ,  $n = 9$ , 5-parameter) over 300 s. Parameter estimates from the curves for 50 and 125 Hz are shown in Table 2. The peak force of the first 500 ms tetanus expressed relative to the maximal force evoked with a 2 s tetanus at 125 Hz was 69% at 30 Hz ( $n = 4$ ), 84% at 50 Hz ( $n = 5$ ) and 96% at 125 Hz ( $n = 9$ ). Dashed vertical line indicates 100 s.

**Table 2.** Parameter estimates obtained by fitting double-sigmoid models to the fatigue profiles evoked with repeated tetani in soleus and EDL muscles

	Soleus		EDL
	50 Hz	125 Hz	125 Hz
<b>First sigmoid</b>			
$\tau_1$ (s)	$4.3 \pm 0.4$	$6.2 \pm 0.2$	$0.5 \pm 0.1\ddagger$
$n_1$	$2.4 \pm 0.5$	$1.7 \pm 0.4$	$1.4 \pm 0.8$
$S_1$ (%·s <sup>-1</sup> )	$-1.2 \pm 0.7$	$-0.8 \pm 0.1$	$-6.7 \pm 4.1\ddagger$
$F_o$ (%)	$91.5 \pm 0.5$	88.9	$90.7 \pm 0.9$
<b>Second sigmoid</b>			
$\tau_2$ (s)	$89.6 \pm 1.0^*$	$54.1 \pm 0.2$	$13.0 \pm 0.1\ddagger$
$n_2$	$3.2 \pm 0.1$	$2.0 \pm 0.03$	$2.5 \pm 0.02$
$S_2$ (%·s <sup>-1</sup> )	$-0.45 \pm 0.02^*$	$-0.58 \pm 0.01$	$-4.09 \pm 0.06\ddagger$
$F_{min}$ (%)	$41.6 \pm 0.5^*$	$26.4 \pm 0.3$	$5.6 \pm 0.1\ddagger$
<b>Statistics</b>			
$r^2$	0.99973	0.99996	0.99999
$MS_e$ (%)	0.61	0.17	0.03
	( $n = 5$ )	( $n = 9$ )	( $n = 13$ )

Parameter estimates are mean values  $\pm$  s.e.m. of  $n$  muscles. Stimulation protocol was 50 or 125 Hz for 500 ms, once every second for 300 s in soleus or 100 s in EDL. Supramaximal pulses (20 V, 0.1 ms) and plate electrodes were used. The parameter estimates and fitting statistics were obtained using the mean data obtained with the six-parameter model (eqn (3)) except for soleus muscles stimulated at 125 Hz, where a five-parameter model was used with  $F_o$  fixed at 88.9% (eqn (4)). Note that  $\tau_1$  and  $\tau_2$  are the half-times for the decay of the first and second sigmoids, respectively. The value of  $\tau_1$  for EDL (0.5 s) implies that the half-time resides midway between the first two tetani. \* Significantly different at 50 and 125 Hz in soleus (Student's unpaired  $t$  test);  $\ddagger$  significantly different at 125 Hz between soleus and EDL (Student's unpaired  $t$  test).

between 90% decay of the first sigmoid and 10% decay of the second sigmoid. The two sigmoids were found to overlap by 97 s for the six-parameter model, whereas with 50 Hz stimulation the sigmoids were separated by 35 s (consistent with the existence of a plateau phase). Hence, the six-parameter estimate of  $F_o$  at 125 Hz cannot be attributed purely to the early processes that occur at 50 Hz, but must reflect the encroachment of processes described by the second sigmoid. Refitting the 125 Hz data using the five-parameter double-sigmoid model (with  $F_o = 88.9\%$ ) generated a convincing fit (Table 2), and with parameter values thought to reflect better the early fatigue process(es) (Dahlstedt *et al.* 2000). With this five-parameter model substitution, the effect of increasing the stimulation frequency from 50 to 125 Hz on the parameter estimates was significant only for the second sigmoid (smaller values of  $\tau_2$  and  $F_{min}$  and greater  $S_2$ , Table 2). Note that for fatigue induced with 125 Hz tetani a double-sigmoid expression was again the superior fitting model according to AIC (Table 1).

When the inter-tetanus rest period was increased from 0.5 to 1.5 s (using repeated fatigue runs in the same soleus

muscles, with 100 tetani at 125 Hz for 500 ms), early fatigue was similar but differences appeared during late fatigue;  $FI_{100}$  increased from  $32 \pm 4\%$  with 0.5 s rest to  $57 \pm 3\%$  ( $n = 4$ ) with 1.5 s rest. The fatigue profile with tetani separated by 1.5 s rest periods remained adequately fitted ( $r^2 = 0.99999$ ,  $MS_{\varepsilon} = 0.08\%$ ) by a six-parameter double sigmoid with  $F_o = 92.8 \pm 0.65\%$ .

When the pulse strength is 4.4 V (0.1 ms) in our experimental set-up, soleus muscles are excited via nerve terminals as opposed to being excited simultaneously over the surface membrane as occurs with 20 V (0.1 ms) pulses (see Cairns *et al.* 2007, for details). Figure 4 shows representative fatigue profiles evoked with repeated short tetani (125 Hz) via the surface membrane (Fig. 4A) or via the nerve terminal in the same soleus muscle (Fig. 4B). These profiles reveal subtle differences during late fatigue, detected between 35 and 65 s of stimulation, and were explored further by curve-fitting (Fig. 4C). The fitting parameters and derived values for the second sigmoid quantitatively reveal differences during late fatigue. Phase III was more rapid at 4.4 V;  $\tau_2$  was reduced significantly from  $46.4 \pm 1.0$  to  $36.7 \pm 0.6$  s, while  $S_2$  increased from  $-1.07 \pm 0.06$  to  $-1.74 \pm 0.10\% s^{-1}$ . Application of eqn (10) revealed that the 20–80% decay time for the second sigmoid increased from 27 s at 4.4 V to 53 s at 20 V. Clearly, our fitting approach can detect subtle changes to the fatigue profile.

### Influence of muscle type on fatigue and recovery profiles

The fibre-type composition details of soleus and EDL muscles, typical of those used throughout the present study, are shown in Table 3.

**Fatigue profile.** Figure 5 shows a representative fatigue run of 100 tetani evoked at 125 Hz for 500 ms once every second in an individual EDL muscle with both original force records and the best-fitting curve (Fig. 5A and B, respectively). Parameter estimates arising from the average fatigue profile of 13 EDL muscles are shown in Table 2. Once again, a double sigmoid was confirmed as the expression of best fit (Table 1). A characteristic feature of fatigue in EDL is a decline of peak force to  $93.1 \pm 0.6\%$  ( $n = 13$ ) by the second tetanus. In contrast, soleus muscle maintained peak force within 2% of its maximal value for  $3.5 \pm 0.1$  tetani ( $n = 32$ ). The times for the 90% decline of the first sigmoid and 10% decline of the second sigmoid in EDL show a separation of 3 s rather than the overlap detected in soleus at 125 Hz. Application of eqn (10) revealed that the first sigmoid was 95% complete after five tetani in EDL and 15 tetani in soleus. The rates and extents of the second sigmoid for each muscle type are shown in Table 2. The 10–90% decay time for the second sigmoid was 26 s in EDL and 123 s in soleus.

Several features of fatiguing stimulation, other than of peak force *per se*, differed between muscle types (see Figs 4A and 5A). First, fade during a 500 ms tetanus appeared during severe fatigue in EDL. This fade escalated from  $\sim 33$  s and continued to progress to a value of  $0.53 \pm 0.06$  ( $n = 13$ ) at 100 s, by which time peak force had already reached a final plateau. In contrast, there was no evidence of fade in any of 32 soleus muscles examined.

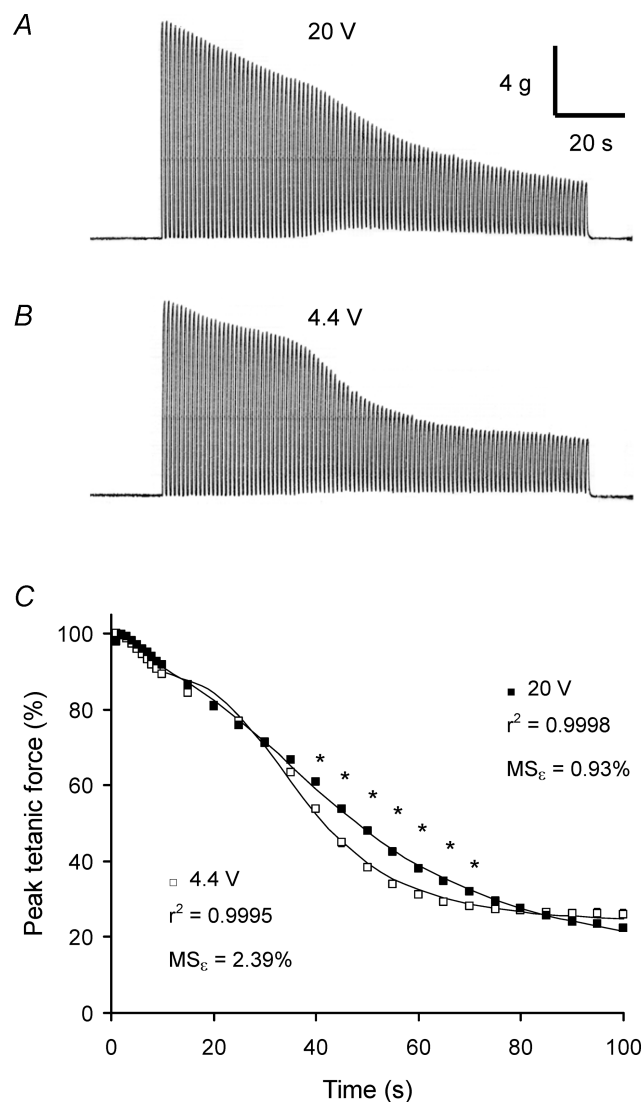


**Figure 4.** Influence of intermittent tetanic stimulation via nerve terminals or simultaneously over the surface membrane of the sarcolemma on the fatigue profile in soleus muscles

Stimulation protocol was 125 Hz for 500 ms, once every second for 100 s. Stimulation pulses (0.1 ms) were evoked with plate electrodes. Original force records are given when stimulating with 20 V pulses, i.e. via the sarcolemma (A), or with 4.4 V pulses, i.e. via nerve terminals (B). Fatigue in B was recorded 154 min after A in the same muscle.

C, the averaged data for peak tetanic force as a function of stimulation time ( $n = 6$ , ■ 20 V and □ 4.4 V), were fitted by five-parameter double-sigmoid models. \* Significant differences (ANOVA). The peak force of a 500 ms tetanus relative to the maximal force evoked with a 2 s tetanus at 125 Hz was 93% at 20 V and 88% at 4.4 V ( $n = 6$ ).

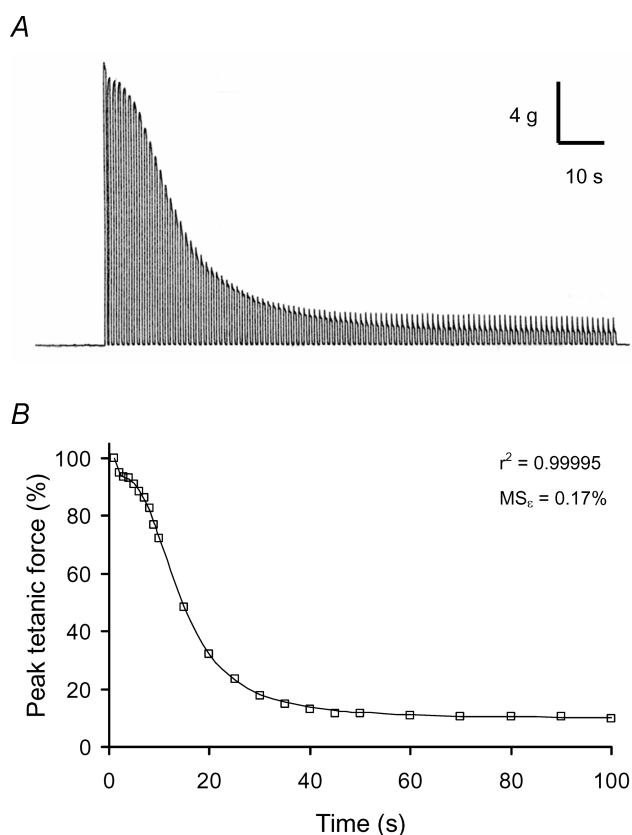
**Table 3. Histochemical and morphological characteristics of mouse soleus and EDL muscles**

Characteristic	Soleus	EDL
Type I (relative fibre area, %)	51.0 ± 1.9 (45–61)	0.7 ± 0.2 (0.1–2.6)
Type IIA or IIX (relative fibre area, %)	49.0 ± 1.9 (45–55)	31.4 ± 3.4 (16–59)
Type IIB (relative fibre area, %)	0.1 ± 0.1 (0–0.3)	67.9 ± 3.5 (41–84)
Total fibres per muscle	523 ± 29	512 ± 46
Total fibre area (mm <sup>2</sup> )	0.602 ± 0.100	0.595 ± 0.105

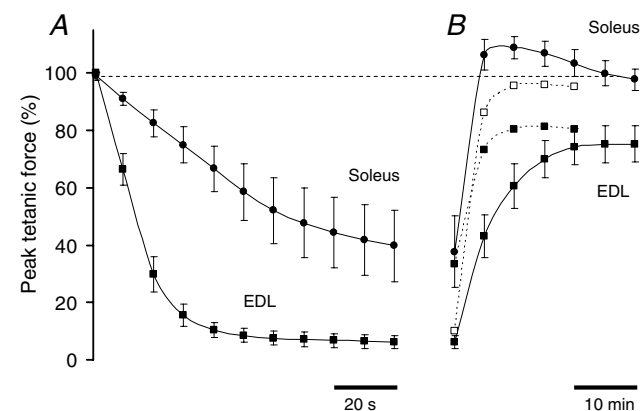
Data are mean values ± s.e.m. (range) of eight soleus and 12 EDL muscles from both hindlimbs of six female Swiss CD-1 mice. Fibre-types were classified by myosin ATPase activity. Note that only three of eight soleus muscles contained type IIB fibres and all EDL muscles contained a few type I fibres. Muscle length was 13.1 ± 1.2 mm for EDL and 10.6 ± 1.1 mm for soleus. Muscle dry weight was 2.56 ± 0.20 mg for EDL and 1.68 ± 0.25 mg for soleus. Some EDL data have been previously used by Robinson & Loiselle (2002).

Second, the resting force between tetani increased in soleus after ~23 s and reached a maximum of 7.9 ± 0.9% ( $n = 32$ ) of peak tetanic force. This effect appeared to be linked to a slowing of the tail of relaxation after the tetanus. The time for complete relaxation increased from less than 500 ms (first tetanus) to 1480 ± 130 ms for the hundredth tetanus in soleus ( $n = 26$ ), although the half-relaxation

time did not change significantly (data not shown). Resting force did not increase during fatigue in EDL or in soleus with longer rest periods when relaxation was complete prior to the following tetanus. Third, in non-fatigued muscle, there was post-tetanic potentiation of twitches by 18.2 ± 1.6% ( $n = 9$ ) in EDL and a post-tetanic depression of twitches by 3.8 ± 0.7% ( $n = 11$ ) in soleus. After fatigue with 100 tetani, the peak twitch force was reduced to about one-half in both muscle types. However, after 20 tetani in EDL, which causes similar fatigue to 100 tetani in soleus, twitch potentiation (32.5 ± 14.7%,  $n = 3$ ) was observed together with a large reduction of tetanic force. Fourth, EDL muscles exhibited significantly less fatigue over 4–20 s

**Figure 5. Representative fatigue run evoked with repeated brief tetani in an individual EDL muscle**

Stimulation protocol was 125 Hz for 500 ms, once every second for 100 s. Supramaximal pulses (20 V, 0.1 ms) and plate electrodes were used. *A*, original force records. *B*, double-sigmoid (6-parameter) model fitted to the peak force data in *A*.

**Figure 6. Influence of intermittent tetanic stimulation on fatigue (A) and recovery profiles (B) in soleus (●) and EDL muscles (■)**

Stimulation protocol was 125 Hz for 500 ms, once every second for 100 s. Supramaximal pulses (20 V, 0.1 ms) and plate electrodes were used. Shown are mean values ± s.d., with data given every 10 s during the fatigue run ( $n = 32$  for soleus and 13 for EDL) and every 5 min during recovery ( $n = 25$  for soleus and 13 for EDL). In *B*, the dotted line with filled squares are the recovery data in EDL after 20 repeated tetani at 125 Hz ( $n = 5$ ), and the dotted line with open squares are the recovery data in EDL after continuous stimulation at 125 Hz for 20 s ( $n = 7$ ), with error bars omitted for clarity. All relative force data points ( $t > 1$  s) during fatigue and recovery were significantly different between soleus and EDL (ANOVA).

during the second fatigue run compared with the first; the largest difference in peak tetanic force was  $10.3 \pm 1.8\%$  ( $n = 9$ ) after 10 tetani. In contrast, the fatigue profile in soleus was largely reproducible when using multiple fatigue runs. For example, there was only a 3–4% greater loss of force over 65–100 s on the second fatigue run.

**Recovery profile.** When investigating fatigue, it is imperative to distinguish between reversible and irreversible loss of force. To that end, we quantified the extent of peak force recovery following a fatigue run. Recovery after 100 tetani was slower and incomplete in EDL compared with that in soleus (Fig. 6B); at 5 min post-fatiguing stimulation, peak force was fully restored in soleus but was still only 43% of its initial value in EDL. The maximal recovery in EDL, to  $79 \pm 2\%$  of initial force ( $n = 13$ ), occurred at 20–25 min. After a fatigue run evoked with 20 tetani in EDL, the peak force had recovered maximally in 10 min (Fig. 6B) but was still incomplete;  $83 \pm 7\%$  of initial force ( $n = 5$ ). Surprisingly, the recovery of force was rapid and complete after a prolonged tetanus in EDL, reaching  $97.8 \pm 0.7\%$  ( $n = 7$ ) of initial force within 10 min (Fig. 6B). Another feature of recovery was a transient augmentation of peak tetanic force in soleus. The maximal increase was to  $108.5 \pm 0.9\%$  of initial force ( $n = 26$ ) in 10–15 min. Thereafter, force reverted to  $97.1 \pm 0.7\%$  of its initial value after  $\sim 60$  min. Similar extents of potentiation occurred after 20 tetani (to  $109.1 \pm 1.0\%$ ,  $n = 4$ ) and 300 tetani (to  $106.7 \pm 1.3\%$ ,  $n = 9$ ).

## Discussion

### Curve-fitting to the fatigue profile

We have shown that many profiles of severe fatigue in mouse skeletal muscles are exceptionally well described mathematically as a double-sigmoid function (as confirmed by the very small values of mean square error,  $MS_e$ ). Such fitting (Figs 1, 3, 4 and 5) was achieved for data arising from intermittent stimulation in both soleus and EDL muscles (125 Hz for 500 ms once every second for 100 or 300 s), and in soleus with repeated tetani evoked at 50 Hz, with rest periods of 1.5 s, or with excitation via nerve terminals. Moreover, the double-sigmoid model gave a better fit, as judged by the smallest Akaike Information Criterion values (Burnham & Anderson, 1998) and smallest residual errors (Fig. 1), than did either single-exponential or single-sigmoidal models (Table 1). Hence, the early fatigue kinetics in particular are much better described by such an analytical descriptor. Moreover, examination of the fatigue literature reveals numerous examples of apparent double-sigmoidal behaviour in several animal species as well as in human muscles (Burke *et al.* 1973; Binder-MacLeod *et al.* 1998;

Chin & Allen, 1998; Ward *et al.* 1998; Chen *et al.* 2001; Ding *et al.* 2002; Cairns *et al.* 2004). Clearly, its occurrence in motor units (Burke *et al.* 1973) and human muscle *in situ* (Binder-MacLeod *et al.* 1998; Ding *et al.* 2002) indicates that it is a common phenomenon and is not restricted to isolated mouse muscles at 25°C. Indeed, our description of the fatigue profile supports but extends the description of Lännergren & Westerblad (1991) by including a final force plateau (phase IV).

Two main advances are conferred by using the double-sigmoid modelling. First, the process is sufficiently rigorous and detailed to quantify the multiple phases of fatigue by extracting the distinct rates and extents of each sigmoid (Table 2). It thus provides a tool to quantify fatigue kinetics in different muscle types, with various stimulation protocols, and for studies where specific phases of fatigue may change, for example with altered ion composition (Cairns *et al.* 1998, 2003, 2004), pharmacological interventions (Gong *et al.* 2003; Kristensen *et al.* 2006) or physical training (Troup *et al.* 1986). The investigation of fatigue properties in knockout or transgenic animals is increasingly centred on isolated muscles from mice (Dahlstedt *et al.* 2000; Nagaraj *et al.* 2000; Chen *et al.* 2001; Gong *et al.* 2003) where our quantification tool can readily be applied. Second, the model provides a temporal separation, into early and late components, of the processes that cause fatigue. The parameter estimates obtained from fitting can therefore reflect the time course and extent of the dominant underlying processes, without implying that only one process is necessarily responsible for each sigmoid. The double-sigmoid curve-fitting approach can therefore be used to standardize the parameters used to characterize fatigue in a variety of models of severe fatigue.

The fitting procedures are straightforward to perform using either eqn (3) or eqn (4) and SAS (or Excel) statistical software, for those fatigue models in which the following criteria are met. First, the fatigue run should be extended so that force loss is severe. A counter-example provided in the present study is given by fatigue induced at 30 Hz in soleus where there is no late fatigue (Fig. 3). Second, near-maximal contractions are required because potentiation of submaximal contractions can influence the fatigue profile (Rankin *et al.* 1988; Bevan *et al.* 1992; Rabischong & Chavet, 1997). Third, excessively high stimulation frequencies and/or very brief rest periods should be avoided in order to diminish the risk of early and late fatigue processes overlapping (and thereby, producing comparable values of  $\tau_1$  and  $\tau_2$ ). Fourth, there must be sufficient data to allow discrimination of the four phases of fatigue, since information is lost if the data are too sparse (compare Fig. 6A with Figs 4 and 5). Fifth, fitting parameters are best obtained from the first fatigue run, since they can change with repeated fatigue runs, especially in fast-twitch muscle. Sixth, the  $MS_e$  should

be reported as a fitting statistic, rather than merely  $r^2$ , since it conveys more informatively the extent of scatter of the observed data around the line-of-best-fit. A notable common fatigue profile, which is not of double-sigmoidal form, involves an initial peak force augmentation followed by a decline to a final plateau, and this seems to be a feature of fatigue induced with submaximal tetani in fast-twitch muscle or motor units (Rankin *et al.* 1988; Bevan *et al.* 1992; Boom *et al.* 1993; Mizrahi *et al.* 1997; Rabischong & Chavet, 1997). The initial potentiation, which most probably masks detection of phases I and II, is not observed when the stimulation elicits high force levels (Bevan *et al.* 1992), which matches our second criterion.

### Fatigue and recovery profiles in soleus and EDL muscles

The myosin ATPase classification of fibre-type (Table 3) confirms that the soleus and EDL muscles used in the present study are heterogeneous, and of similar compositions to those described elsewhere (Crow & Kushmerick, 1982; Kushmerick *et al.* 1992; Chin *et al.* 2003; Thabet *et al.* 2005). The important muscle-type differences were that soleus contained 51% slow-twitch type I fibres and virtually no fast-twitch type IIB fibres, whereas EDL contained 68% type IIB fibres and <1% type I fibres. Mouse soleus and EDL muscles both contain other fast-twitch fibres that can only be distinguished as type IIA or type IIX based on myosin heavy chain isoform assays (Kushmerick *et al.* 1992; Thabet *et al.* 2005). The muscle types have similar total fibre areas (Table 3), which suggests that differences in fatigue profile are unlikely to be ascribable to differences in diffusion distances for fatigue factors such as oxygen insufficiency (Barclay, 2005) or the accumulation of ions or metabolites.

**Early fatigue (first sigmoid).** The rationale for applying a double-sigmoid expression to both muscle types is that the early fatigue process(es) are assumed to be common in soleus and EDL, with only the kinetics being different. Phase I was considerably briefer in EDL than in soleus (smaller  $\tau_1$ , Table 2), being 95% complete in five tetani in EDL and 34 tetani in soleus. The difference in time course occurred, first, because fatigue processes were manifested after just one tetanus in fast-twitch muscle (Fig. 5A; Chin & Allen, 1998), in contrast to taking three or four tetani in soleus and, second, because the maximal rate of force decline was 8.4-fold greater in EDL than soleus (larger  $S_1$ ; Table 2). Phase II is indicated by  $F_o$  whose values were comparable in EDL and soleus; 90.7 and 88.9% ( $P = 0.48$ ), respectively. Hence, the magnitude of early fatigue,  $(100 - F_o)$ , was  $\sim 10\%$  in both muscle types.

A strong candidate to cause early fatigue is inorganic phosphate ( $P_i$ ; Dahlstedt *et al.* 2000), which rapidly

accumulates as creatine phosphate is consumed. Certainly,  $P_i$  can build up within 1–3 s in EDL, where the rate of  $P_i$  accumulation is three- to fourfold greater than in soleus (Crow & Kushmerick, 1982). This may explain the greater value of  $S_1$  for EDL than soleus (Table 2). Also,  $P_i$  has been shown to increase to  $\sim 15$  mM in soleus at the end of a fatigue protocol similar to ours and to even higher levels in EDL (Dahlstedt *et al.* 2000). Similar values of  $[P_i]$  reduce maximal cross-bridge function by 5–20% in skinned fibres (Fryer *et al.* 1995; Potma *et al.* 1995; Debold *et al.* 2004), which is in line with the decline of  $F_o$  by  $\sim 10\%$  in both muscle types (Table 2). Moreover, post-tetanic twitch potentiation occurred after a single tetanus and with severe fatigue after 20 tetani in EDL, thought to be due to phosphorylation of myosin light chains (Tubman *et al.* 1996), and this may counteract early fatigue in fast-twitch fibres. Notably, knockout mice which cannot accumulate  $P_i$  do not exhibit a phase I (Dahlstedt *et al.* 2000).

**Late fatigue (second sigmoid).** Phase III had a shorter time course in EDL than in soleus (smaller  $\tau_2$ , Table 2), primarily because of the 7.1-fold greater maximal rate of force decline in EDL (larger  $S_2$ , Table 2). In close agreement is the  $\sim$ eightfold greater rate as assessed by straight-line regression in rat EDL and soleus (Clausen *et al.* 2004). Phase IV (or  $F_{\min}$ ) was lower in EDL than in soleus at 125 Hz (Table 2). Therefore, the extent of late fatigue,  $(F_o - F_{\min})$ , amounted to 83% of initial force in EDL and 63% of initial force in soleus.

A notable experimental finding was that the second sigmoid, which occurs with repeated tetani at 50 or 125 Hz (for 500 ms every 1 s), was completely prevented over 100 s at the lower frequency of 30 Hz in soleus (Fig. 3). The magnitude of late fatigue at 100 s,  $(F_o - FI_{100})$ , amounted to 53% of the initial force at 125 Hz, but was attenuated to 25% at 50 Hz and abolished at 30 Hz. Thus, late fatigue is entirely frequency dependent, at least over the 30–125 Hz range in slow-twitch muscle. Table 2 provides more details, showing that phase III occurs earlier at 125 than at 50 Hz;  $\tau_2$  was abbreviated by 35 s primarily because phase II (which takes  $\sim 28$  s at 50 Hz) is eliminated. There was an additional small contribution from a greater rate of fatigue since  $S_2$  was 30% steeper at 125 Hz (Table 2 and Fig. 3).

We hypothesize that the frequency dependence of late fatigue is mainly a consequence of changes brought about by ion movements during each action potential (Juel, 1986; Lindinger & Heigenhauser, 1988). In line with this proposal, it has been shown that lowered extracellular  $[Na^+]$ ,  $[Ca^{2+}]$  or  $[Cl^-]$  (Cairns *et al.* 1998, 2003, 2004) all hasten the onset of late fatigue during repeated tetani in soleus. Moreover, the magnitude of these ion shifts increases with stimulation frequency (Clausen *et al.* 2004), along with a greater depolarization during trains of stimuli at 125 than at 50 Hz (Cairns *et al.* 2003). Ion shifts may be responsible for diminished sarcolemmal excitability

during similar fatigue protocols (Cairns *et al.* 1998, 2007; Gong *et al.* 2003; Clausen *et al.* 2004), hence lesser  $\text{Ca}^{2+}$  release in late fatigue (Lännergren & Westerblad, 1991; Chin & Allen, 1996, 1998; Ward *et al.* 1998). Furthermore, the slightly greater rate of late fatigue with nerve terminal, compared with sarcolemmal, stimulation (Fig. 4) may be attributed to an earlier loss of excitability in the surface membrane or an extra contribution from impaired neuromuscular transmission.

Several contractile properties other than peak force differ between muscle types during late fatigue (Figs 4A and 5A). First, fade characteristically develops during phase IV in EDL but not in soleus; hence, the constancy of peak force does not necessarily imply that all processes have reached a steady state. Second, resting force increases in soleus, but not in EDL, when short inter-tetanus rest periods are used (Cairns *et al.* 1998; Dahlstedt *et al.* 2000; Gong *et al.* 2003) and is attributed to a slowing of the late phase of relaxation. Third, post-tetanic potentiation of twitches occurs simultaneously with tetanus depression in fatigued EDL, as sometimes described for other fast-twitch muscles (Rankin *et al.* 1988; Tubman *et al.* 1996). Fourth, with multiple fatigue runs, the profile is largely reproducible in soleus but not in EDL muscles. In contrast, EDL displays greater resistance to fatigue during phase III on a repeat fatigue run (Helander *et al.* 2002), which is possibly due to a potentiating process (Tubman *et al.* 1996; Helander *et al.* 2002) or as a consequence of inappropriate normalization to a lowered initial force following incomplete recovery from the first fatigue run.

**Recovery.** The recovery of peak force after repeated tetani was slower and incomplete in EDL so that a deficit of ~20% remained (Fig. 6B). This prolonged impairment was similar after 20 or 100 tetani and comparable to that seen after repeated tetani in other fast-twitch preparations (Chin & Allen, 1996, 1998; Dahlstedt *et al.* 2000; Nagaraj *et al.* 2000; Helander *et al.* 2002; Gong *et al.* 2003), but, remarkably, contrasts with the full recovery observed after a continuous tetanus (Fig. 6B). Apparently, intermittent stimulation allows an extra force-depressing process to occur in fast-twitch fibres, which seems to depend on glucose (Helander *et al.* 2002) and may involve a mechanism causing long-term impairment of  $\text{Ca}^{2+}$  release from the SR (Chin & Allen, 1996; Dahlstedt *et al.* 2000; Nagaraj *et al.* 2000). Peak force recovers faster and completely in soleus (Fig. 6B), possibly due to faster restoration of ion gradients with greater activity of  $\text{Na}^+$ – $\text{K}^+$  pumps in slow-twitch than in fast-twitch fibres (Juel, 1986; Clausen *et al.* 2004).

The transient augmentation of peak tetanic force during recovery in soleus (Fig. 6B) was of similar magnitude (~10%) to that observed previously (Bruton *et al.* 1997). It is unlikely to involve phosphorylation of myosin light chains (Tubman *et al.* 1996), which is thought to

cause post-tetanic potentiation of twitches, or glycogen supercompensation (Helander *et al.* 2002), since both of these processes also occur in fast-twitch muscle which does not display recovery potentiation (Fig. 6B). A potential mediator is lowered  $[\text{P}_i]$  since the resting  $[\text{P}_i]$  of ~5 mM in mouse soleus (Crow & Kushmerick, 1982; Kushmerick *et al.* 1992) can fall by one-half after several tetani (Bruton *et al.* 1997), which could contribute to a 10–15% increase of maximal cross-bridge function (Fryer *et al.* 1995; Potma *et al.* 1995). The lack of recovery potentiation in EDL (Fig. 6B) could be explained by the lower resting  $[\text{P}_i]$  of ~1 mM in mouse EDL (Kushmerick *et al.* 1992), thereby providing rather limited scope for further reductions of  $[\text{P}_i]$  after fatigue.

## Conclusion

A double-sigmoid model provides an exceptionally good fit to a variety of fatigue profiles and is therefore a useful method to quantify fatigue kinetics in many, although not all, models of severe fatigue in isolated muscles from mice. It should be particularly useful when applied to investigation of mechanisms of fatigue following molecular biology interventions.

## References

- Barclay CJ (2005). Modelling diffusive  $\text{O}_2$  supply to isolated preparations of mammalian skeletal and cardiac muscle. *J Musc Res Cell Motil* **26**, 225–235.
- Bevan L, Laouris Y, Reinking RM & Stuart DG (1992). The effect of the stimulation pattern on the fatigue of single motor units in adult cats. *J Physiol* **449**, 85–108.
- Binder-MacLeod SA, Lee SCK, Russ DW & Kucharski LJ (1998). Effects of activation pattern on human skeletal muscle fatigue. *Muscle Nerve* **21**, 1145–1152.
- Boom HBK, Mulder AJ & Veltink PH (1993). Fatigue during functional neuromuscular stimulation. *Prog Brain Res* **97**, 409–418.
- Bruton JD, Wretman C, Katz A & Westerblad H (1997). Increased tetanic force and reduced myoplasmic  $[\text{P}_i]$  following a brief series of tetani in mouse soleus muscle. *Am J Physiol Cell Physiol* **272**, C870–C874.
- Burke RE, Levine DN, Tsairis P & Zajac FE (1973). Physiological types and histochemical profiles in motor units of the cat gastrocnemius. *J Physiol* **234**, 723–748.
- Burnham KP & Anderson DR (1998) *Model Selection and Multimodel Inference: A Practical Information-Theoretic Approach*, 2nd edn. Springer, New York. ISBN 0-387-95364-7.
- Cairns SP, Buller SJ, Loiselle DS & Renaud JM (2003). Changes of action potentials and force at lowered  $[\text{Na}^+]_o$  in mouse skeletal muscle: implications for fatigue. *Am J Physiol Cell Physiol* **285**, C1131–C1141.
- Cairns SP, Chin ER & Renaud JM (2007). Stimulation pulse characteristics and electrode configuration determine site of excitation in isolated mammalian skeletal muscle: implications for fatigue. *J Appl Physiol* **103**, 359–368.

- Cairns SP, Hing WA, Slack JR, Mills RG & Loiselle DS (1998). Role of extracellular  $[Ca^{2+}]$  in fatigue of isolated mammalian skeletal muscle. *J Appl Physiol* **84**, 1395–1406.
- Cairns SP, Knicker AJ, Thompson MW & Sjøgaard G (2005). Evaluation of models used to study neuromuscular fatigue. *Exerc Sport Sci Rev* **33**, 9–16.
- Cairns SP, Ruzhynsky V & Renaud JM (2004). Protective role of extracellular chloride in fatigue of isolated mammalian skeletal muscle. *Am J Physiol Cell Physiol* **287**, C762–C770.
- Chen G, Carroll S, Racay P, Dick J, Pette D, Traub I, Vrbova G, Eggl P, Celio M & Schwaller B (2001). Deficiency in parvalbumin increases fatigue resistance in fast-twitch muscle and upregulates mitochondria. *Am J Physiol Cell Physiol* **281**, C114–C122.
- Chin ER & Allen DG (1996). The role of elevations in intracellular  $[Ca^{2+}]$  in the development of low frequency fatigue in mouse single muscle fibres. *J Physiol* **491**, 813–824.
- Chin ER & Allen DG (1998). The contribution of pH-dependent mechanisms to fatigue at different intensities in mammalian single muscle fibres. *J Physiol* **512**, 831–840.
- Chin ER, Grange RW, Viau F, Simard AR, Humphries C, Shelton J, Bassel-Duby R, Williams RS & Michel RN (2003). Alterations in slow-twitch muscle phenotype in transgenic mice overexpressing the  $Ca^{2+}$  buffering protein parvalbumin. *J Physiol* **547**, 649–663.
- Clausen T, Overgaard K & Nielsen OB (2004). Evidence that the  $Na^+ - K^+$  leak/pump ratio contributes to the differences in endurance between fast- and slow-twitch muscles. *Acta Physiol Scand* **180**, 209–216.
- Crow MT & Kushmerick MJ (1982). Chemical energetics of slow- and fast-twitch muscles of the mouse. *J Gen Physiol* **79**, 147–166.
- Dahlstedt AJ, Katz A, Wieringa BE & Westerblad H (2000). Is creatine kinase responsible for fatigue? Studies of isolated skeletal muscle deficient in creatine kinase. *FASEB J* **14**, 982–990.
- Debold EP, Dave H & Fitts RH (2004). Fiber type and temperature dependence of inorganic phosphate: implications for fatigue. *Am J Physiol Cell Physiol* **287**, C673–C681.
- Ding J, Wexler AS & Binder-Macleod SA (2002). A predictive fatigue model—I: predicting the effect of stimulation frequency and pattern on fatigue. *IEEE Trans Neural Syst Rehabil Eng* **10**, 48–58.
- Fryer MW, Owen VJ, Lamb GD & Stephenson DG (1995). Effects of creatine phosphate and  $P_i$  on  $Ca^{2+}$  movements and tension development in rat skinned skeletal muscle fibres. *J Physiol* **482**, 123–140.
- Gong B, Legault D, Miki T, Seino S & Renaud JM (2003).  $K_{ATP}$  channels depress force by reducing action potential amplitude in mouse EDL and soleus muscle. *Am J Physiol Cell Physiol* **285**, C1464–C1474.
- Helander I, Westerblad H & Katz A (2002). Effects of glucose on contractile function,  $[Ca^{2+}]_i$ , and glycogen in isolated mouse skeletal muscle. *Am J Physiol Cell Physiol* **282**, C1306–C1312.
- Juel C (1986). Potassium and sodium shifts during in vitro isometric muscle contraction, and the time course of the ion-gradient recovery. *Pflügers Arch* **406**, 458–463.
- Kristensen M, Hansen T & Juel C (2006). Membrane proteins involved in potassium shifts during muscle activity and fatigue. *Am J Physiol Regul Integr Comp Physiol* **290**, R766–R772.
- Kushmerick MJ, Moerland TS & Wiseman RW (1992). Mammalian skeletal muscle fibers distinguished by contents of phosphocreatine, ATP, and  $P_i$ . *Proc Natl Acad Sci USA* **89**, 7521–7525.
- Lännergren J & Westerblad H (1991). Force decline due to fatigue and intracellular acidification in isolated fibres from mouse skeletal muscle. *J Physiol* **434**, 307–322.
- Lindinger MI & Heigenhauser GJF (1988). Ion fluxes during tetanic stimulation in isolated perfused rat hindlimb. *Am J Physiol Regul Integr Comp Physiol* **254**, R117–R126.
- Merletti R, Lo Conte LR & Orizio C (1991). Indices of muscle fatigue. *J Electromyogr Kinesiol* **1**, 20–33.
- Mizrahi J, Levin O, Aviram A, Isakov E & Susak Z (1997). Muscle fatigue in interrupted stimulation: effect of partial recovery on force and EMG dynamics. *J Electromyogr Kinesiol* **7**, 51–65.
- Nagaraj RY, Nosek CM, Brotto MAP, Nishi M, Takeshima H, Nosek TM & Ma J (2000). Increased susceptibility to fatigue of slow- and fast-twitch muscles from mice lacking the MG29 gene. *Physiol Genomics* **4**, 43–49.
- Potma EJ, van Graas IA & Stienen GJM (1995). Influence of inorganic phosphate and pH on ATP utilization in fast and slow skeletal muscle fibers. *Biophys J* **69**, 2580–2589.
- Rabischong E & Chavet P (1997). Regression-based indices of fatigue in paraplegics' electrically stimulated quadriceps. *Med Eng Phys* **19**, 749–754.
- Rankin LL, Enoka RM, Volz KA & Stuart DG (1988). Coexistence of twitch potentiation and tetanic force decline in rat hindlimb muscle. *J Appl Physiol* **65**, 2687–2695.
- Robinson DM & Loiselle DS (2002). Effect of creatine manipulation on fast-twitch skeletal muscle of the mouse. *Clin Exp Pharmacol Physiol* **29**, 1105–1111.
- Russ DW, Vandeborne K & Binder-Macleod SA (2002). Factors in fatigue during intermittent electrical stimulation of human muscle. *J Appl Physiol* **93**, 469–478.
- Thabet M, Miki T, Seino S & Renaud JM (2005). Treadmill running causes significant fiber damage in skeletal muscle of  $K_{ATP}$  channel-deficient mice. *Physiol Genomics* **22**, 204–212.
- Troup JP, Metzger JM & Fitts RH (1986). Effect of high-intensity exercise training on functional capacity of limb skeletal muscle. *J Appl Physiol* **60**, 1743–1751.
- Tubman LA, MacIntosh BR & Maki WA (1996). Myosin light chain phosphorylation and posttetanic potentiation in fatigued skeletal muscle. *Pflügers Arch* **431**, 882–887.
- Ward CW, Spangenburg EE, Diss LM & Williams JH (1998). Effects of varied fatigue protocols on sarcoplasmic reticulum calcium uptake and release rates. *Am J Physiol Regul Integr Comp Physiol* **275**, R99–R104.
- Williams JH & Ward CW (1991). Dihydropyridine effects on skeletal muscle fatigue. *J Physiol (Paris)* **85**, 235–238.

## Acknowledgements

We thank Professor Will Hopkins for helpful discussion and Peter Mellow for graphical assistance. This work was supported by a grant from the Lottery Grants Board of New Zealand.